Materials Science and Engineering A223 (1997) 158-167

The Effect of Stress on the Widmanstätten Ferrite Transformation

J. R. Yang
National Taiwan University, Institute of Materials Science and Engineering, Taipei, Taiwan, R.O.C.

L. C. Chang
University of Cambridge JRDC, Department of Materials Science and Metallurgy, Cambridge CB2 3QZ, England, U. K.

Abstract

Transformation of Widmanstätten ferrite has been considered to be displacive with a large shear component (larger than martensite and bainite). It is expected that the external stress exerts a profound effect on Widmanstätten ferrite formation. Optical metallographs show that under the influence of an applied compressive stress (below the yield strength of austenite) the number of crystallographic variants of Widmanstätten ferrite is reduced drastically and there is a strong tendency for the plates that do grow to align. Transformation strains (including longitudinal and radial strains) during Widmanstätten ferrite formation are shown to be consistent with the microstructural changes. Furthermore, transmission electron micrographs clearly reveal that the applied stress leads to the decoupling of the adjacent accommondating plates of Widmanstätten ferrite. All the experimental results are explained in terms of the invariant-plane-strain displacive mechanism for Widmanstätten ferrite.

1. Introduction

Widmanstätten ferrite is an undesirable constituent and its presence leads to poor toughness in low-alloy steels. It has been generally recognised that the transformation of Widmanstätten ferrite can be easily stimulated if the prior austenite grain sizes are very large. For example, Widmanstätten ferrite usually forms in the heat-affected zone and the weld deposit of low-alloy steels. The transformation temperature of Widmanstätten ferrite has been known to be just below that of allotriomorphic ferrite [1,2]. In a typical low-alloy steel weld deposit or heat-affected zone, two kinds of Widmanstätten ferrite commonly exist: primary and secondary Widmanstätten ferrite. Secondary Widmanstätten ferrite nucleates at the allotrimorphic ferrite/austenite boundaries and grows as sets of parallel plates separated by thin regions of austenite, the latter subsequently being retained to ambient temperature or partially transforming to martensite and/or pearlite. On the other hand, primary Widmanstätten ferrite nucleates directly from austenite grain boundaries which are not covered by allotriomorphic ferrite.

On an optical scale, Widmanstätten ferrite possesses a plate shape with thin wedge section. When a pre-polished crystal of austenite is allowed to transform to Widmanstätten ferrite, the tent-like shape change can be observed [3,4]. Under the examination of transmission electron microscope, the Widmanstätten ferrite plates have been generally found to be associated in groups of two adjacent variants in intimate contact. It appears that a single wedge of Widmanstätten ferrite actually consists of a pair of ferrite plates [4]. The adjacent ferrite plates have also been found to be nearly the same crystallographic orientation and to have habit plane pole in close proximity [4]. This phenomenon can be understood as follows. At high temperatures (Widmanstätten ferrite forms at low undercoolings below the Ae_3) it is impossible for the Widmanstätten ferrite plate to grow on its own, since the

strain energy due to shape change would far exceed the available driving force. Hence, the reaction of Widmanstätten ferrite should involve the simultaneous and adjacent co-operative growth of two ferrite plates, which are crystallographic variants whose shape change cancel each other, drastically reducing the strain energy [4].

The formation of Widmanstätten ferrite can be regarded as a deformation mode which consists of two adjacent and opposing invariant-plane strain (IPS) deformations for a single wedge of Widmätten ferrite [4]. These IPS deformations each have a large shear component and imply the existence of an atomic correspondence between the parent and product phases as far as the iron and substitutional solue atoms are concerned. Interstitials atoms, such as carbon, can diffuse during growth of Widmanstätten ferrite without affecting the shape change or the displacive character of the transformation.

During displacive transformation induced by a decrease in temperature, the chemical driving force brings about the deformation. It is nature to expect that an appropriate external stress should have a profound effect on the progress of the Widmanstätten ferrite transformation. Such effects have been observed in many experiments involving both bainitic and martensitic transformations [5-15]. However, so far the related research on Widmanstätten ferrite has not been studied as yet. The main aim of the present work is to investigate how the external stress exerts an influence on the transformation of Widmanstätten ferrite. Furthermore, an up-quench heat treatment has been carried out to cause the transformation of allotriomorphic ferrite after some amounts of Widmanstätten ferrite already forming. As will be seen later, these specific investigations provide good evidence to elucidate the nature of the Widmanstätten ferrite.

2. Experimental method

The experimental steel was made as 20 kg vacuum induction melts using high purity base materials. The ingot was forged and hot rolled into 10 mm diameter rods. The chemical composition of the steel consisted of Fe-0.059C-1.96Si-2.88Mn (wt%). All the thermomechnical treatments were carried out in a Themecmaster thermomechanical simulator. Samples for Thermecmaster were machined from the homogenised steel rods (reaustenitised at 1200^{o}C for 3 days while sealed in quartz tube containing a partial pressure of pure argon) in the form of 8 mm diameter cylindrical rods with 12 mm length. The specimen was heated using r.f. coil and the temperature was measured with a Pt/Pt-10Rh (wt.%) thermocouple. The level of vacuum in the specimen chamber can reach 10^{-5} torr to protect specimens from oxidation during reaustenitisation at high temperatures.

In order to find out a suitable condition of heat treatment for Widmanstätten ferrite formation, a series of isothermal heat treatments has been tested. For the purpose of studying the effect of stress on Widmanstätten ferrite formation, the schemes with and without applying stress have been carried out as follows. After reaustenitisation at 1300^{o}C for 2 min, the specimen was quenched to 565^{o}C by means of a controlled high-pressure argon jet directed axially at the specimen, then held at 565^{o}C for different periors of time from 10 min to 2 h, and finally quenched to ambient temperature. As to the other parallel scheme, 50 MPa stress was applied immediately after the sample reached 565^{o}C during the periors of isothermal transformation.

In an attempt to differential the formation mechanism of Widmastätten ferrite from that of allotriomorphic ferrite, an up-quench heat treatment was carried out to cause the transformation of allotriomorphic ferrite after some amounts of Widmanstätte ferrite already forming. The details of the up-quench treatment are as follows. After reaustenitisation at 1300^{o}C for 2 min followed by isothermal treatment at 565^{o}C for 30 min, the specimens were rapidly up-quenched to

700°C, held at 700°C for a period of time, and finally quenched to ambient temperature.

The specimens for optical metallography were prepared from the thermomechanical simulator samples. The observed section was parallel to the longitudinal direction. The specimens were mechanically polished and then etched in 2% nital solution. Transmission electron microscopy specimens were obtained from 0.25 mm thick discs cut from the thermomechanical simulator samples. The discs were thinned to 0.05 mm by abrasion on silicon carbide papers; the specimens were then twin-jet electropolished using a mixture of 5% perchloric acid, 25% glocerol and 70% ethanol at ambient temperature and 60V polishing potential. They were examined using a Philips EM400T transmission electron microscope operated at 120kV.

3. Results and discussion

The calculated time-temperature-transformation (T-T-T) diagram (presented in Fig.1), based on model developed by Bhadeshia [16], confirms that the chosen transformation temperature (565°C) can cause the growth of Widmanstätten ferrite. The diagram also indicates that the formation of allotriomorphic ferrite may occur before that of Widmänstatten ferrite (i.e., secondary Widmanstätten ferrite forms.) However, it should be noted that this analysis of T-T-T diagram is applied for the usual range of austenite grain sizes. As the prior austenite grain sizes are extremely large, the formation of allotriomorphic ferrite would be retarded and that of Widmanstätten ferrite should be promoted. In this work the treatment of reautenitisation was therefore performed at 1300°C for 2 min.

In order to understand the response of the microstructural feature to the applied stress, the corresponding optical microstructures are illustrated in Fig. 2. It was intended in this work to limit the applied stress to a value below the yield strength of austenite, so that the austenite can elastically support the applied stress prior to transformation. Any plastic deformation can complicate

interpretation because the resulting defect structure can assist or interfere with the progress of transformation. The experiments were carried out at 50 MPa load level, which was well below the yield strength of austenite at 565^{o}C as referred to the related published data [17]. Fig. 2 shows the optical metallographs obtained from the specimens reaustenised at 1300^{o}C for 2 min and then isothermally treated at 565^{o}C for various periods of time (without and with 50MPa applied stress during the isothermal holding); the direction of applied stress is indicated by an arrow on the corresponding metallographs. For the samples isothermally treated at 565^{o}C for 10 min, the corresponding metallographs (Figs 2(a) and 2(b)) display that a thin layer of allotriomorphic ferrite decorated at prior austenite grain boundaries, and that a few amounts of Widmanstätten formed from the allotriomorphic ferrite. At this stage, the effect of applied stress is not yet significant, and the microstructures for the samples without and with applied stress are nearly the same. Figs 2(c) and 2(d) show some amounts of Widmanstätten ferrite obtained from the samples isothermally treated at 565^{o}C for 30 min. Under the free stress condition, several crystallographic variants of Widmanstätten ferrite occur within the prior austenite grain (Fig. 2(c)); while, in the applied stress circumstance, one specific crystallographic variant of Widmanstätten ferrite appears to be greater in number (Fig. 2(d)). As the specimens isothermally treated at 565^{o}C for 1 and 2h (Figs 2(e) - 2(h)), where large amounts of Widmanstatten ferrite can be obtained, a main crystallographic variant of Widmanstätten ferrite was definitely dominant within the prior austenite grain in the samples with the applied stress (Figs 2(f) and 2(h)). Furthermore, the metallograph (Fig. 2(h)) also indicates that the plates of Widmänstatten ferrite can grow extremely long under the influence of applied stress.

The measurements of transformation strains are illustrated in Fig.3. The longitudinal and radial strains were recorded during isothermal transformation, and referred only to the strains caused by transformation. In the absence of

applied stress(as shown in Fig. 3(a)), both the longitudinal and radial strains were positive, and they had nearly the same trend. Their rates were initially rapid but decreased with time. For the applied stress (50 Mpa) condition, the strains were of opposite sign; the longitudinal strain became negative, whereas the radial strain was postive (as prsented in Fig. 3(b)). At the beginning the change rates of radial strain was much faster than that in the free stress condition. It implies that the stress can accelerate kinetics of the Widmanstätten ferrite formation.

The trends of transformation strains (Fig. 3) and microstructural changes (Fig. 2) can be interpreted on the basis of invariant-plane-strain (IPS) displacive transfromation mechanism as follows. Without any applied stress, in a random polycrystalline sample, the transformation strains can only be isotropic, because the shear componts of IPS randomly oriented plates would tend to cancel out, and also because the dilatational componts would appear to be a uniform volume expansion. When a compressive stress (which is below the yield stress of austenite) is applied during the isothermal transformation of Widmanstätten ferrite, the dilatational components of IPS would be suppressed, but the shear components would interact favourably. The compressive-stress resolves to give maximum shear stresses on planes which lie nearly at 45^{o} to the stress axis. Widmanstätten ferrite variants which happen to be most parallel to those planes are expected to be favoured by the stress, and will form preferentally. This is the reason why the aligned microstructure was developed (Figs 2(d), 2(f) and 2(h)). Since the favoured variant of Widmanstätten ferrite dominates, the strains are therefore always of opposite sign. The result is analogous to that for bainitic transformation under the influence of stress [15]. The experiments provide strong evidence of the shape deformation accompanying the displacive growth of Widmanstätten ferrite.

Previous studies [3,4] have indicated that the transformation of Widmanstätten ferrite is displacive with a large shear component (about 0.4, larger than

martensite and bainite). Judging from these reasearch, it appears that the microstructral change induced by transformation under the influence of stress is expected to be very pronounced. Fig. 4 shows a high magnification metallograph obtained from the same specimen for the corresponding metallograph of Fig. 2(h). It displays a clear microstructure response; under the application of stress the plates of Widmanstätten ferrite grow to align and become extremely long. The detailed microstructural observation by transmission electron microscopy is relevant and illustrated in Figs 5 - 10. Electron micrographs of Figs 5 and 6 obtained from the specimens without applied stress isothermally treated at 565^{o}C for 30 min and 1 h respectively; they show that a single wedge of Widmanstätten ferrite actually consists of a pair of ferrite plates. The observations are consistent with those reported in the previous study [4]. On the other hand, the single plates of Widmanstätten ferrite are usually found on isothermally transforming with the applied stress for 30 min and 1 h respectively (as shown in Figs 7 and 8). Furthermore, a striking feature (Figs 9 and 10) can also be found in the samples isothermally treated with applied stress for 2 h. The transformation electron micrographs reveal that after a single plate of Widmanstätten ferrite growth, subsequent single plates are sympathetically nucleated near the tip of their prior plates, and eventually the plates form a sheaf-like morphology. Electron diffraction confirmed that the plates within the sheaf structure were in approximately the same crysrallographic orientation. The detailed microstructural observation provide strong evidence suggesting that the applied stress leads to the decoupling of the adjacent accommindating plates of Widmanstätten ferrite. Because the application of stress can boost the overall driving force with the mechanical driving force to overcome the strain energy due to shape change, the formation of single plate of Widmanstätten consequently becomes possible. Under the influence of stress, that single plates of Widmanstätten ferrite can develop the sheaf-like structure also reflects the nature of displacive transformation [14].

The dislocation densities of Widmanstätten ferrite for the samples without and with applied stress have been estimated using transmission electron microscopy. A series of micrographs was taken in bright field under two-beam conditions (as presented in Figs 11 and 12). Each dislocation density determination was based on measurements from ten micrographs, taken at magnification of 40,000. The details of dislocation densities measurements have been presented elsewhere [18]. The complete experimental data are listed in Table 1 and 2. The average corrected dislocation densities of Widmanstätten ferrite, obtained from the samples isothermally treated without and with applied stress, are (2.58±1.12) x 10^{14} and (3.01±0.58) x 10^{14} m^{-2} respectively. The values are approximately the same and slightly lower than those of acicular ferrite and bainite [18,19].

In order to distinguish the formation mechanism of Widmanstätten ferrite from that of allotriomorphic ferrite, the specimens were reaustenitised at 1300^{o}C for 2 min, then isothermally transformed at 565^{o}C for 30 min, and immediately rapidly up-quenched to 700^{o}C for isothermal transformation of allotriomorphic ferrite. The Microstructural observations are illustrated in Figs 13 and 14. The wedge morphology of Widmanstätten ferrite plates became wave-shaped (Fig. 13(a)), as isothermal transformation at 700^{o}C for 10 min. The Widmanstätten ferrte/austenite interfaces were degenerated into a series of perturbations (Fig.13(b)), when isothermal transformation at 700^{o}C for 30 min. The detailed morphology of perturbations has been examined under the observation of transmission electron microscope. Fig. 14(a) reveals that the small ferrite grain growed at the original Widmanstäten ferrite/austenite interface and caused the interface to bulge out. The ferrite corresponding to the perturbations was found to be in the same crystallographic orientation as Widmanstätten ferrite. Whereas, Fig.14(b) show that the migration tread of the wedge during the ferrite transformation led to a ragged contour. The results clearly show that the development of perturbations, which accomplish diffusional transformation to ferrite, destroys the characteristic wedge shape of

Widmanstätten ferrite. The result is similar to the case, in which the difussional transformation of austenite → ferrite after bainite forming leads to the development of perturbations from the bainite/austenite interfaces [20]. It provides strong evidence showing that Widmanstätten ferrite is not a diffusional product.

4. Conclusions

The isothermal transformation of Widmanstätten ferrite under the influence of applied stress (below the yield strength of austenite) has been investigated. The metallographs show that the growth of Widmanstätten ferrite responds remarkably to the applied stress. This consequently brings about the development of aligned microstructure. The measured strains during transformation are also consistent with the microstructural changes. In addition, the evidence of transmission electron micrographs clearly indicates that the applied stress leads to the decoupling of the adjacent accommondating plates of Widmanstätten ferrite; i.e., the back-to-back growth of mutually accommodating plates is not favoured in this case. Furthermore, the results of up-quench treatment show that the diffusional transformation of ferrite destroys the characteristic morphology of Widmanstätten ferrite. All the results can only be interpreted in terms of the invariant-plane-strain displacive mechanism for Widmanstätten ferrite.

Acknowledgments

The authors are grateful to the National Science Council, Taipei, Taiwan, ROC for financial support and to Professor Colin Humphreys for the provision of laboratory facilities. HKDHB's contribution was under the auspices of the "Atomic Arrangements: Design and Control Project" which is a collaborative venture between the University of Cambridge and the Research and Development Corporation of Japan.

References

1. H. K. D. H. Bhadeshia, L. -E. Svensson and B. Gretoft, Acta Metall., 33(1985)1271.
2. E. Levine and D. C.Hill, Met. Trans. A, 8(1977)1453.
3. J. D Watson and P.G. McDougall, Acta Metall., 21(1973)961.
4. H. K. D. H. Bhadeshia, Acta Metall., 29(1981)1117.
5. J. R. Patel and M. Cohen, Acta Metall., 1(1953)531.
6. H. K. D. H. Bhadeshia, J. Mater. Sci., 17(1982)383.
7. G. B. Olson, in " Encyclopedia of Materials science and Engineering" edited by R. W. Chan (Pergamon, Oxford, 1986) P.2929.
8. C. M. Wayman, in "Physical Metallurgy" edited by R. W. Chan and P. Haasen (North-Holland, Amsterdam, 1983) P.1031.
9. H. K. D. H. Bhadeshia, Scripta Metall., 14(1980)821.
10. R. Freiwilling, J. Kudrman and P. Chraska, Met. Trans. A, 7(1976)1091.
11. M. Umemoto, S. Bando and I. Tamura, in " Proceedings of the international conference on martensitic transformations", Tokyo, The Japan Institute of Metals, 1986, P.595.
12. H. K. D. H. Bhadeshia, S. A. david, J. M. Vitek and R. W. Reed, Mater. Sci. Technol., 7(1991) 686.
13. H. K. D. H. Bhadeshia, " Bainite in Steels" (the Institute of Materials London, 1992) P. 210.
14. S. S. Babu and H. K. D. H. bhadeshia, Mater. Sci. Eng., A156 (1992) 1.
15. A. Matsuzaki H. K. D. H. Bhadeshia and H. Harada, Acta Metall., 42(1994)1081.
16. H. K. D. H. Bhadeshia, Met. Sci., 16(1982)159.
17. I. Weiss, J. J. Jonas and G. E. Ruddle, in " Process Modelling Tools", edited by J. F. Thomas, Jr. (American Society for Metals, OH,1981).
18. J. R. Yang and H. K. D. H. Bhadeshia, America Welding Journal, 69(1990) 305s.

19. H. K. D. H. Bhadeshia and J. W. Christian, Metall. Trans.A, 21(1990)767.

20. H. K. D. H. Bhadeshia, in " Proc. of Int. Conf. on Solid → Solid Phase Transformations", Pittsburgh, ASM, Metal Park, OH, 1981, p.1041.

Figure captions

Fig. 1 Calculated TTT Diagram, Based on model developed by Bhadeshia [16], for the experimental steel.

Fig. 2 Optical metallographs showing the development of Widmanstätten ferrite for the specimens isothermally treated at 565°C for various periods of time. The direction of applied stress indicated by the arrow. (a) 10 min without stress; (b) 10 min with stress; (c) 30 min without stress; (d) 30 min with stress; (e) 1 h without stress; (f) 1 h with stress; (g) 2 h without stress; (h) 2 h with stress.

Fig. 3 Plot of the radial (R) and longitudinal (L) strains as a function of time during isothermal transformation: (a) without stress; (b) with stress.

Fig. 4 A high magnification metallograph showing the microstructure of Widmanstätten ferrite for the corresponding metallograph of Fig. 2(h).

Fig. 5 Transmission electron micrograph, obtained from a stress-free sample, showing that a single wedge of Widmanstätten ferrite consists of a pair of ferrite plates.

Fig. 6 Transmission electron micrograph, obtained from a stress-free sample, showing the back-to-back growth of two mutually accommodating Widmanstätten ferrite plates.

Fig. 7 Transmission electron micrograph showing the single plate of Widmanstätten ferrite morphology in the sample isothermally treated at 565°C (with the applied stress) for 30 min.

Fig. 8 Transmission electron micrograph showing the single plate of Widmanstätten ferrite morphology in the sample isothermally treated at 565°C (with the applied stress) for 1 h.

Fig. 9 Transmission electron micrograph showing that after a single plate (Plate A) growth, subsequent single plate (Plate B) forms near the tip of the prior plate.

Fig. 10 Transmission electron micrograph showing that after a single plate (Plate A) growth, subsequent single plates (Plates B and C) are sympathetically nucleated near the tip of their prior plates, and a sheaf-like morphology eventually forms. (a) Bright field image; (b) corresponding diffraction patterns for Plates A, B and C respectively.

Fig. 11 Transmission electron micrograph showing a bright field image of Widmanstätten ferrite (obtained from the stress-free sample), taking using approximately two-beam condition.

Fig. 12 Transmission electron micrograph showing a bright field image of Widmanstätten ferrite (obtained from the sample with applied stress), taking using approximately two-beam condition.

Fig. 13 Optical metallographs showing that wedge morphology of Widmanstätten ferrite has become wave-shaped (a), and that degenerated into perturbations (b).

Fig. 14 Transformation electron micrographs (a) and (b) revealing the degenerated interface structures for the corresponding optical metallograph of Fig. 13 (b).

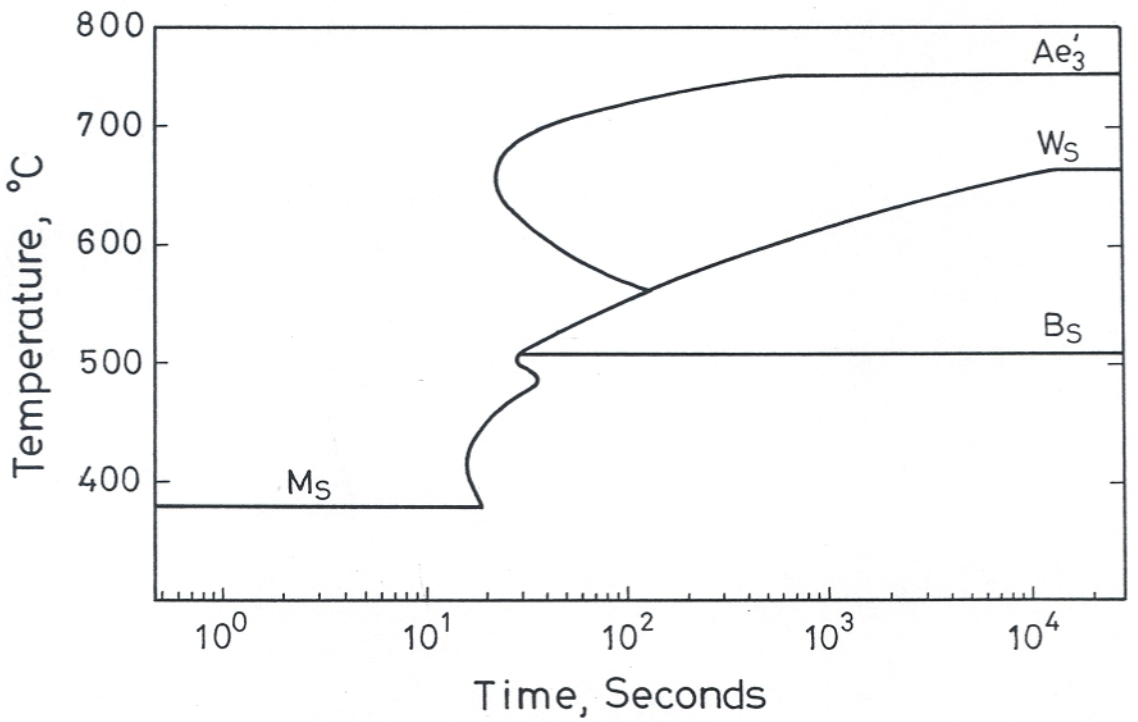

Fig. 1 Calculated TTT Diagram, Based on model developed by Bhadeshia [16], for the experimental steel.

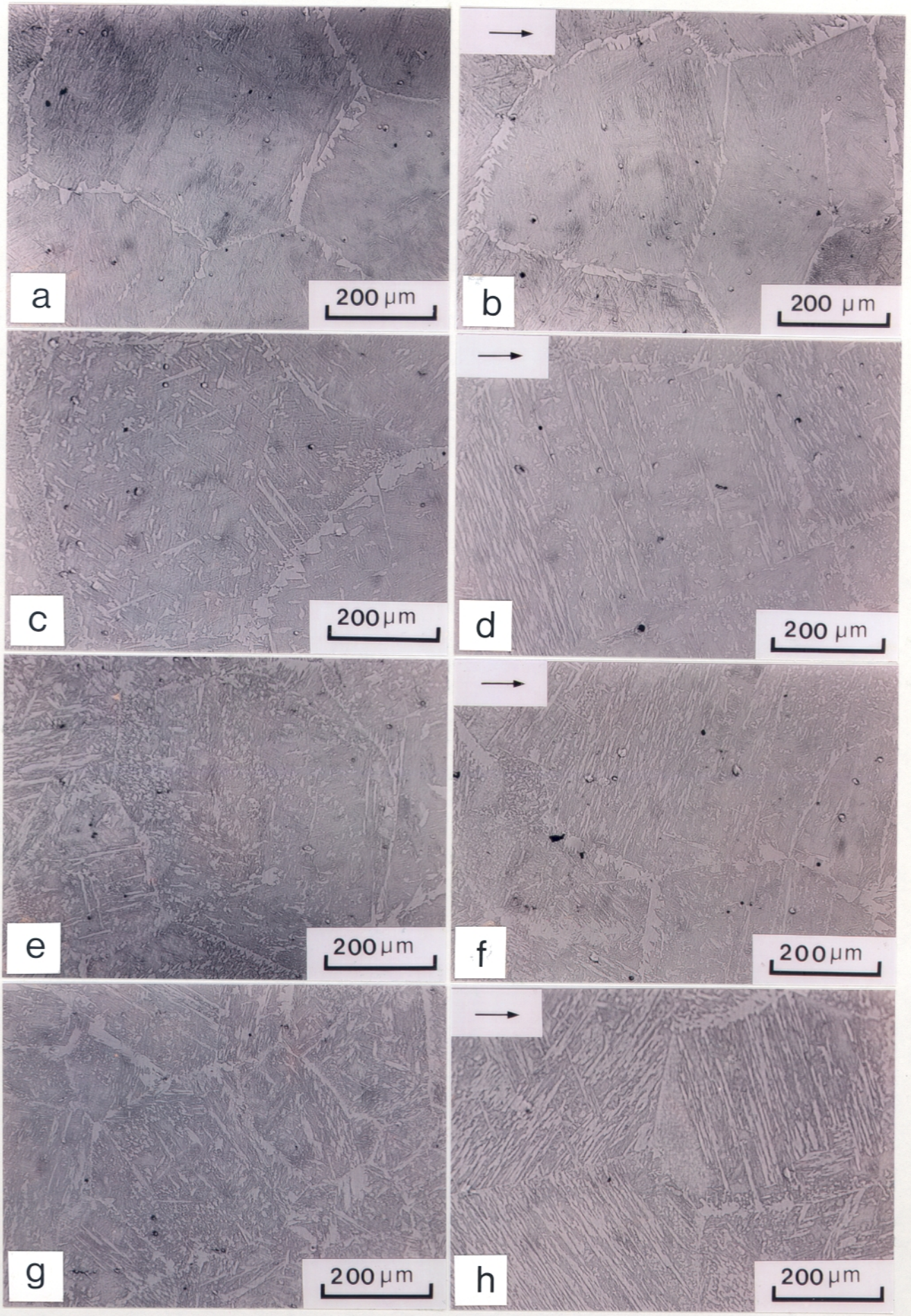

Fig. 2 Optical metallographs showing the development of Widmanstätten ferrite for the specimens isothermally treated at 565°C for various periods of time. The direction of applied stress indicated by the arrow. (a) 10 min without stress; (b) 10 min with stress; (c) 30 min without stress; (d) 30 min with stress; (e) 1 h without stress; (f) 1 h with stress; (g) 2 h without stress; (h) 2 h with stress.

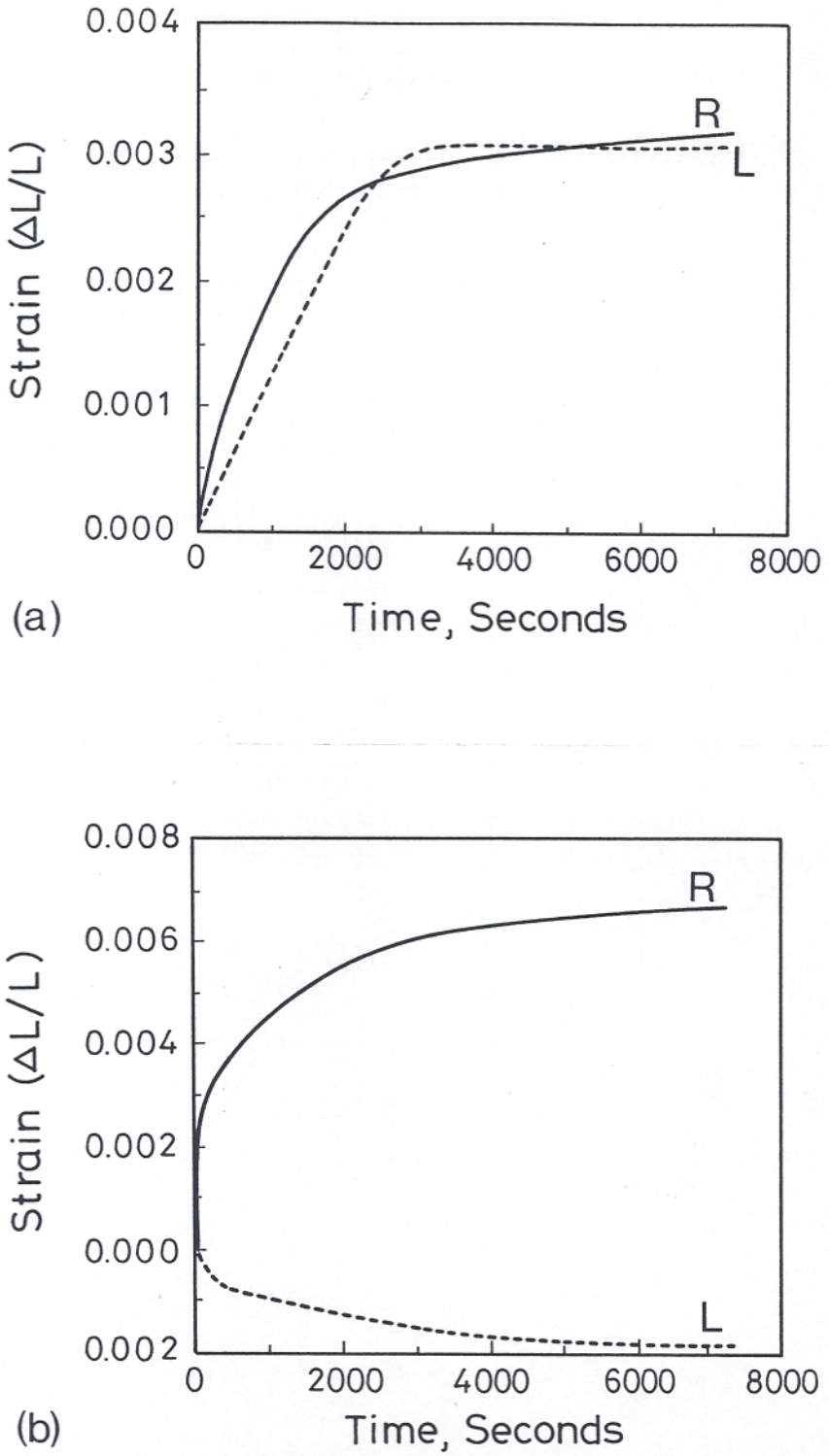

Fig. 3 Plot of the radial (R) and longitudinal(L) strains as a function of time during isothermal transformation: (a) without stress; (b) with stress.

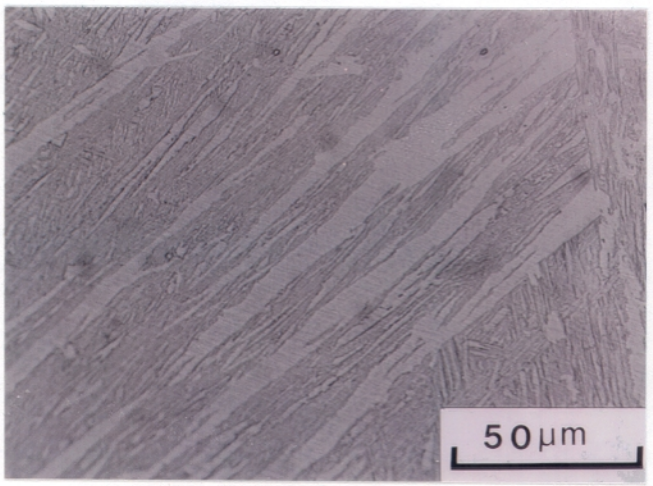

Fig. 4 A high magnification metallograph showing the microstructure of Widmanstätten ferrite for the corresponding metallograpy of Fig. 2(h).

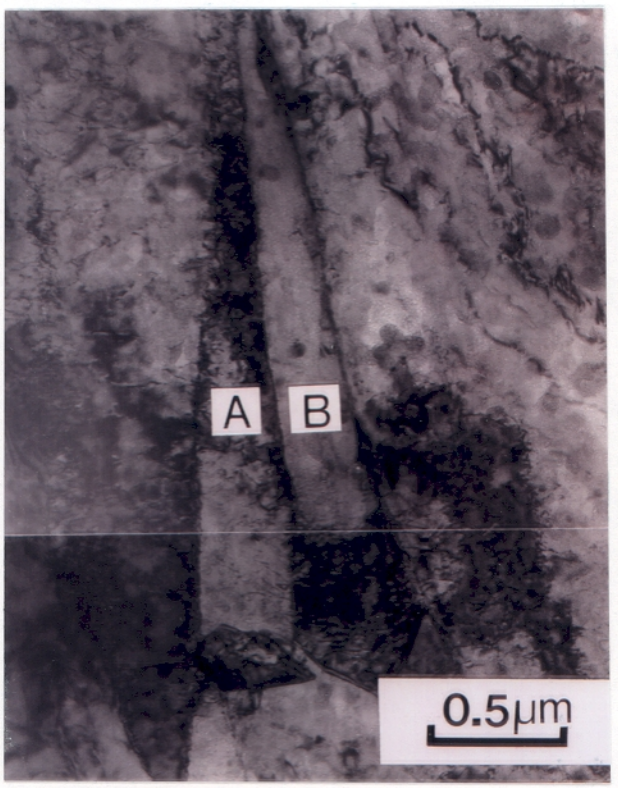

Fig. 5 Transmission electron micrograph, obtained from a stress-free sample, showing that a single wedge of Widmanstätten ferrite consists of a pair of ferrite plates.

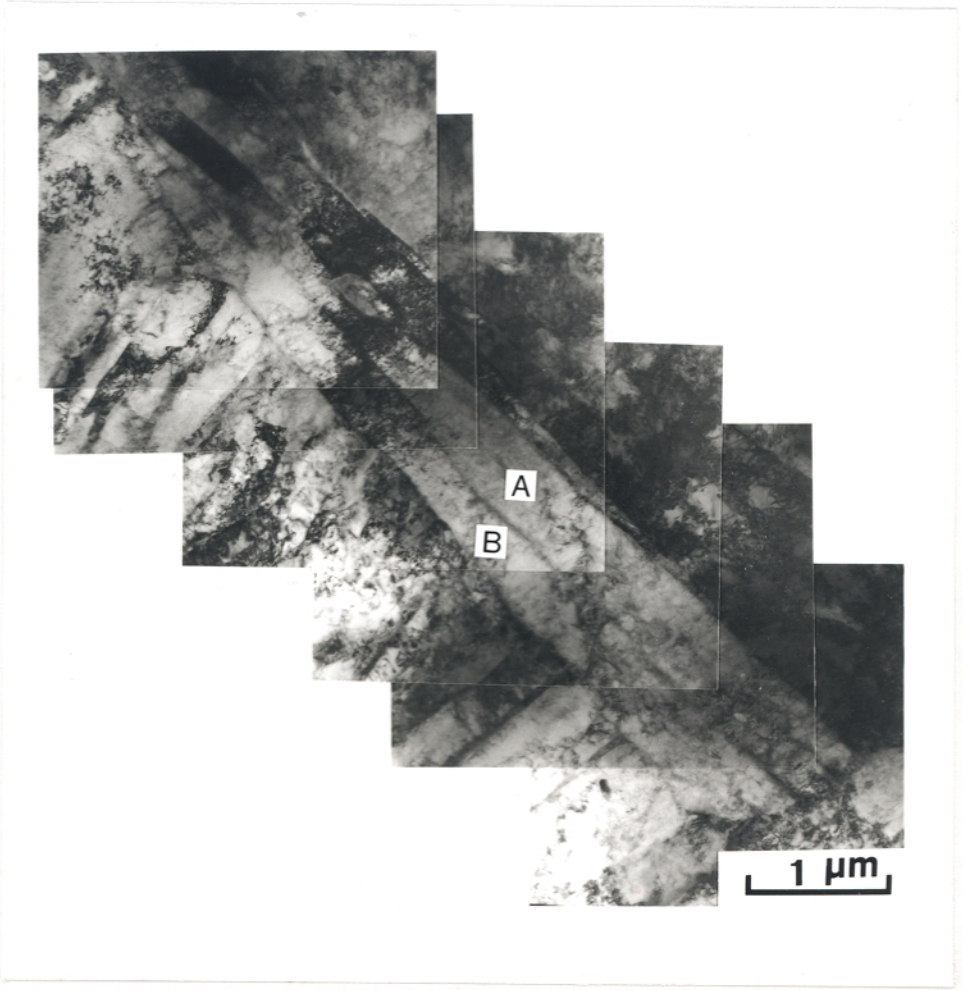

Fig. 6 Transmission electron micrograph, obtained from a stress-free sample, showing the back-to-back growth of two mutually accommodating Widmanstätten ferrite plates.

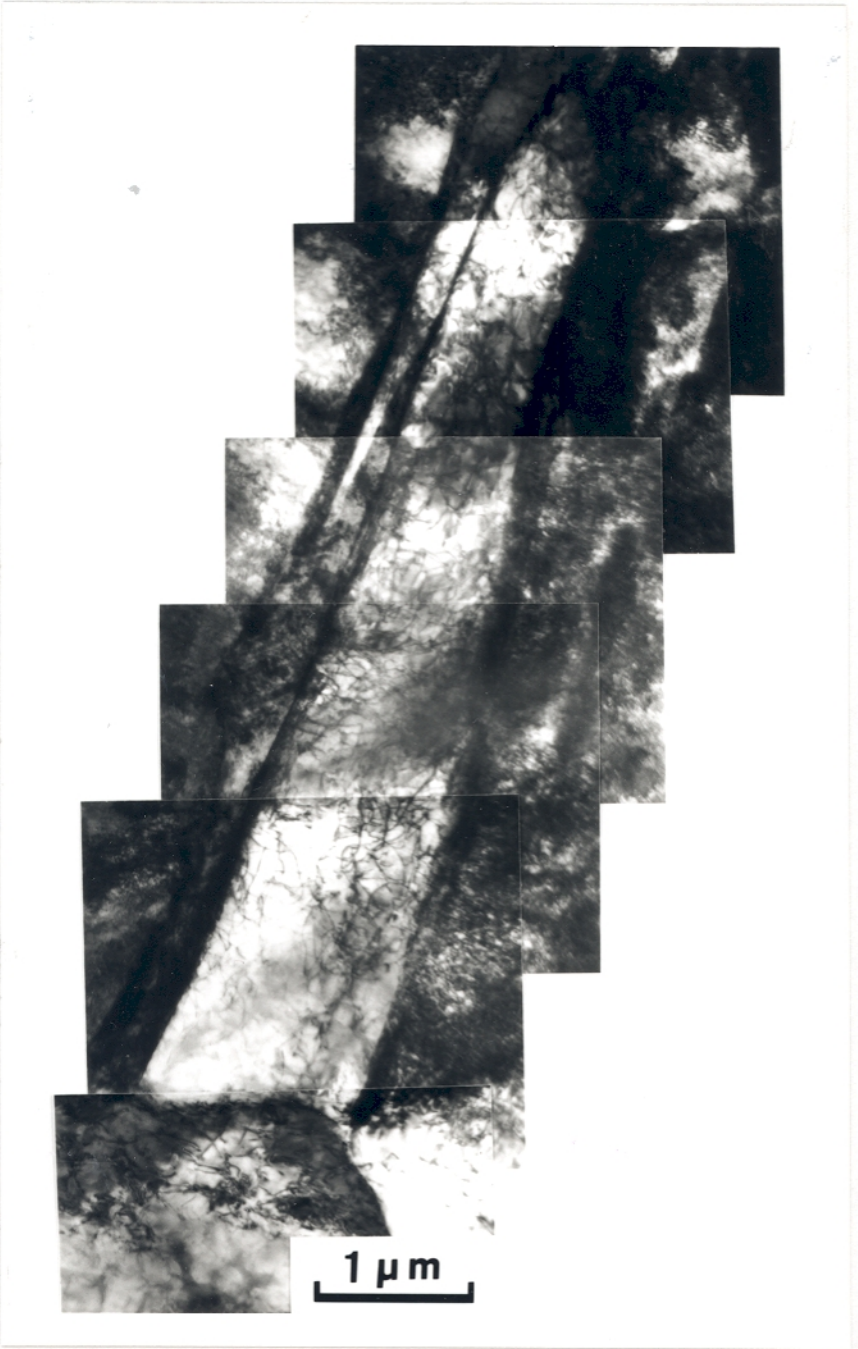

Fig. 7 Transmission electron micrograph showing the single plate of Widmanstätten ferrite morphology in the sample isothermally treated at 565°C (with the applied stress) for 30 min.

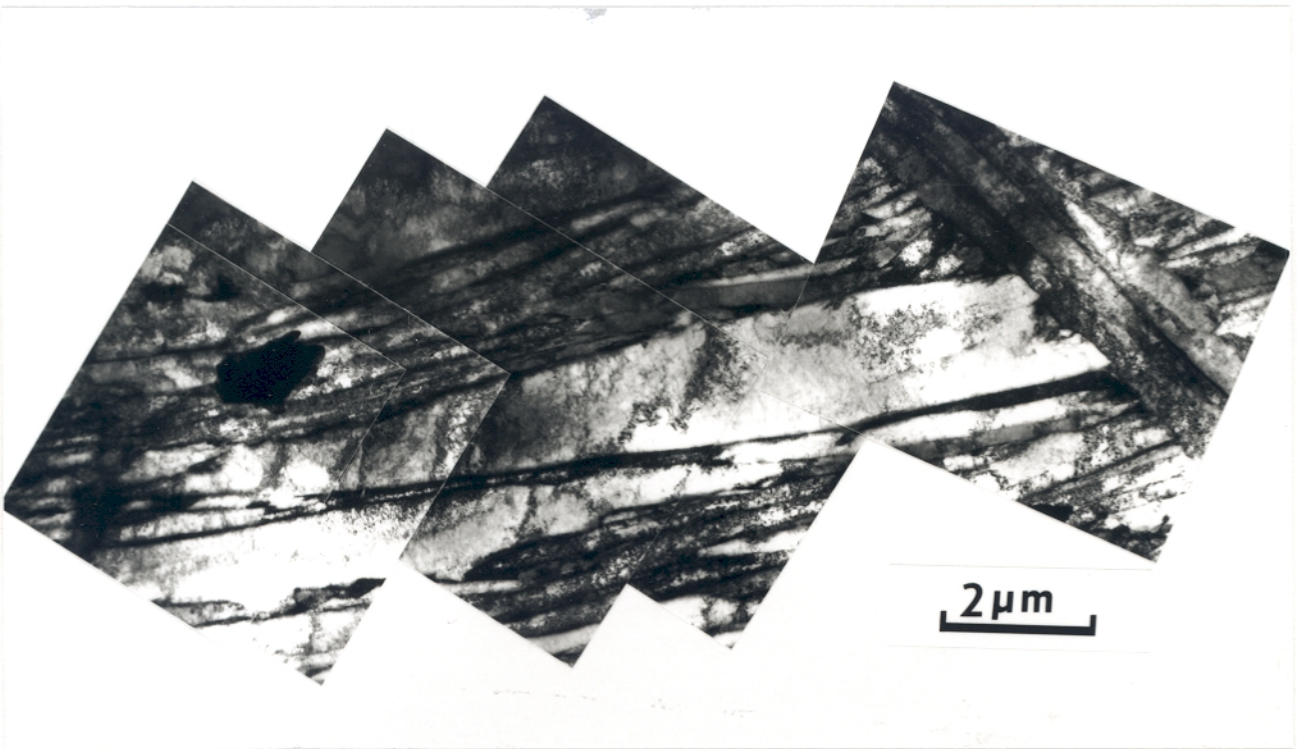

Fig. 8 Transmission electron micrograph showing the single plate of Widmanstätten ferrite morphology in the sample isothermally treated at 565°C (with the applied stress) for 1 h.

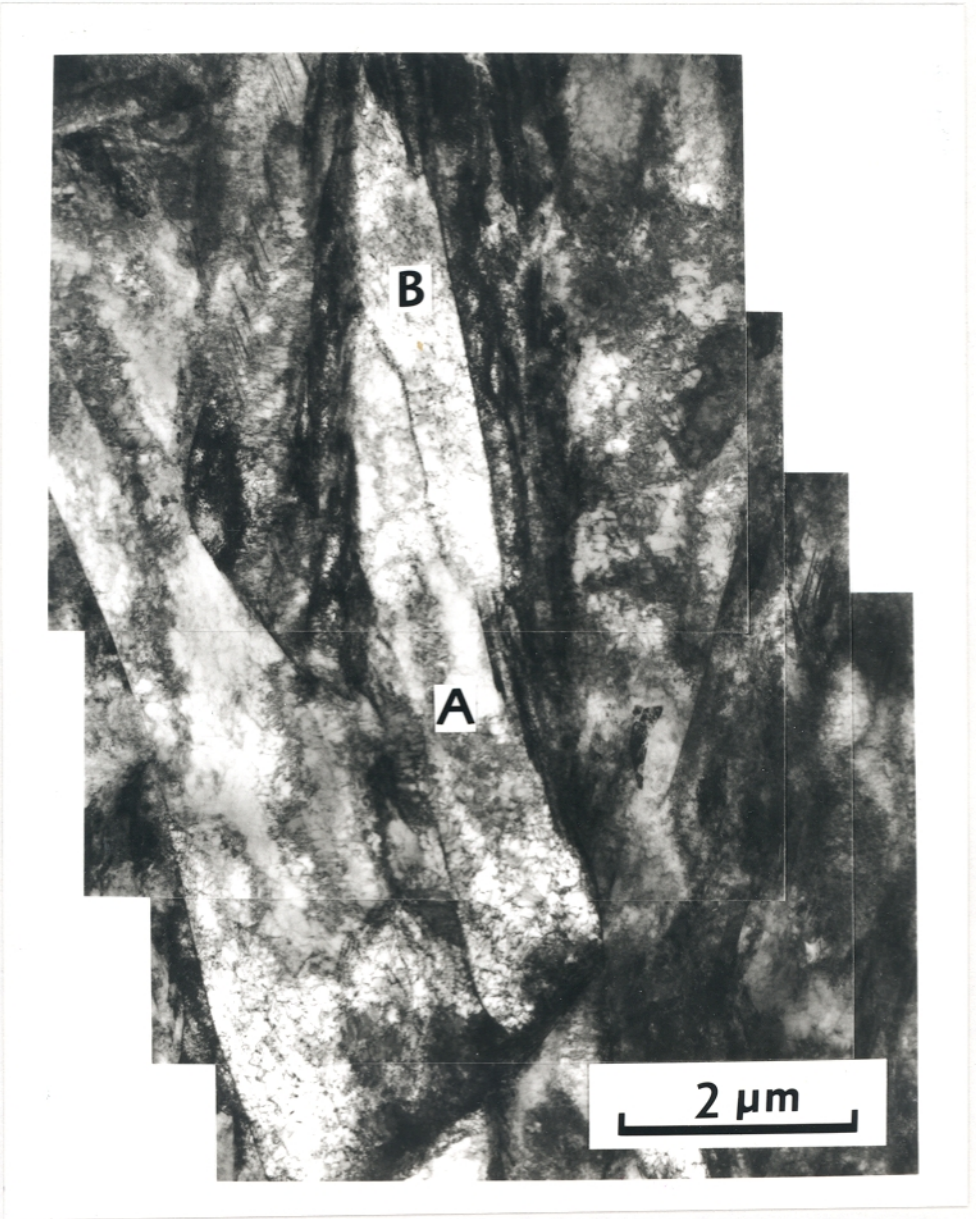

Fig. 9 Transmission electron micrograph showing that after a single plate (Plate A) growth, subsequent single plate (Plate B) forms near the tip of the prior plate.

.

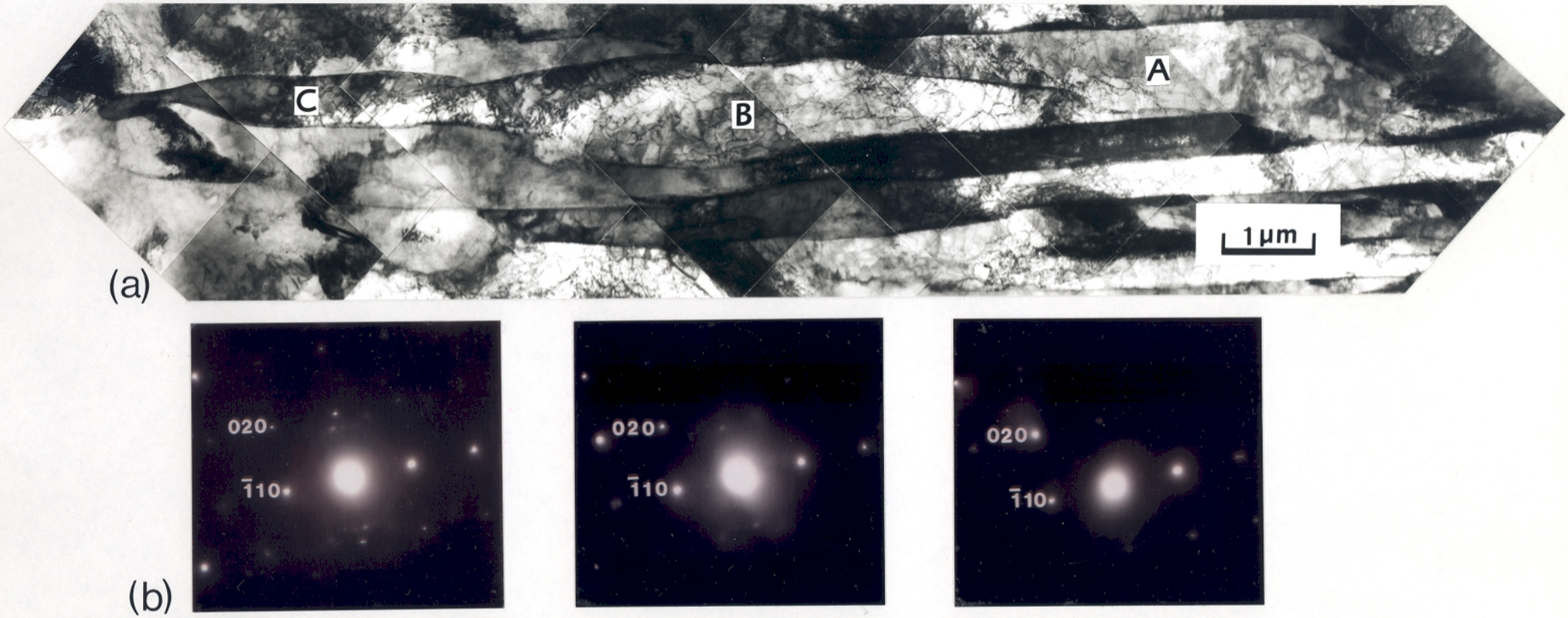

Fig. 10 Transmission electron micrograph showing that after a single plate (Plate A) growth, subsequent single plates (Plates B and C) are sympathetically nucleated near the tip of their prior plates, and a sheaf-like morphology eventually forms. (a) Bright field image; (b) corresponding diffraction patterns for Plates A, B and C respectively.

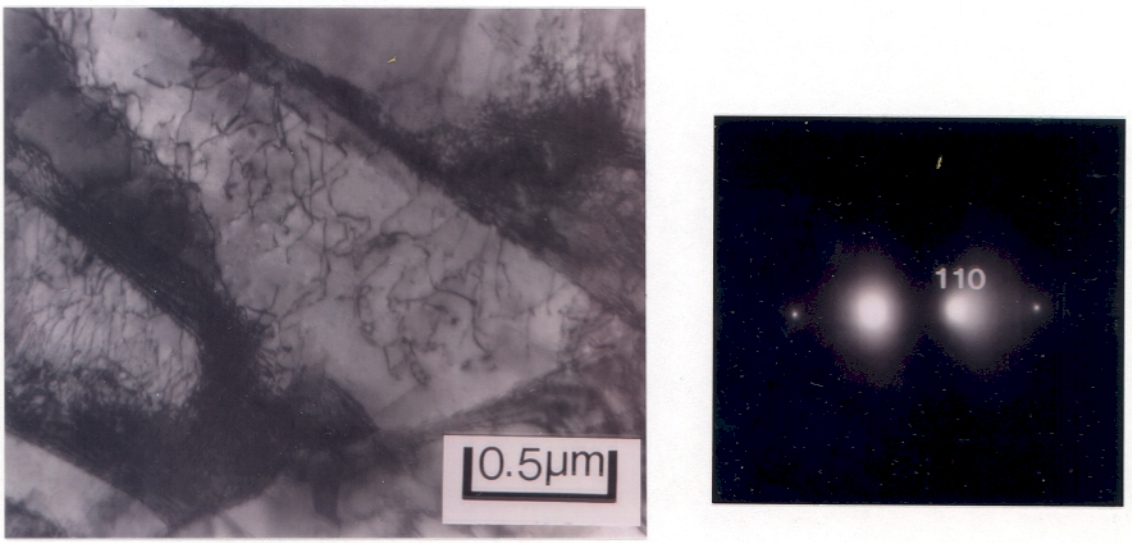

Fig. 11 Transmission electron micrograph showing a bright field image of Widmanstätten ferrite (obtained from the stress-free sample), taking using approximately two-beam condition.

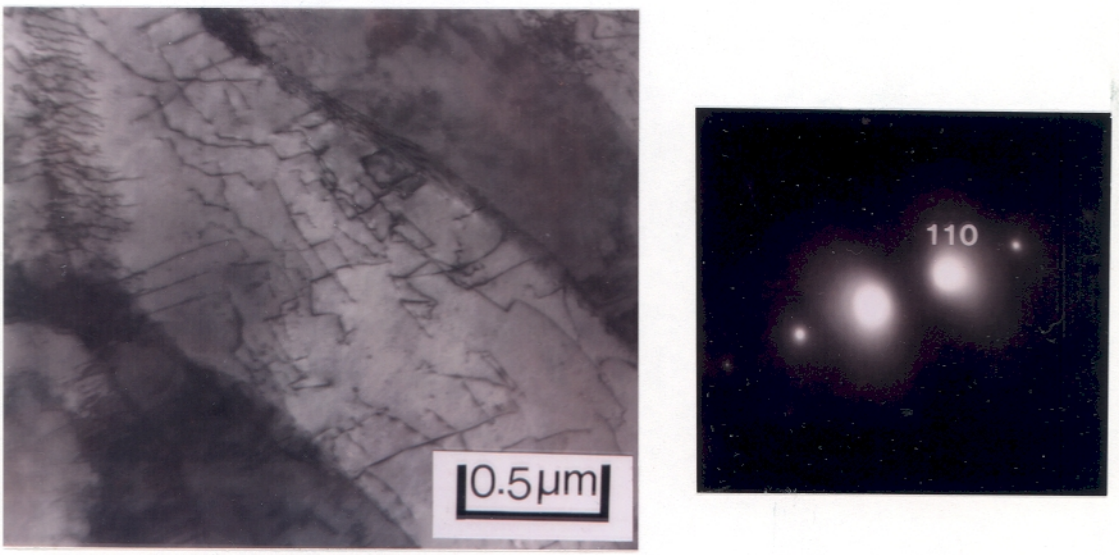

Fig. 12 Transmission electron micrograph showing a bright field image of Widmanstätten ferrite (obtained from the sample with applied stress), taking using approximately two-beam condition.

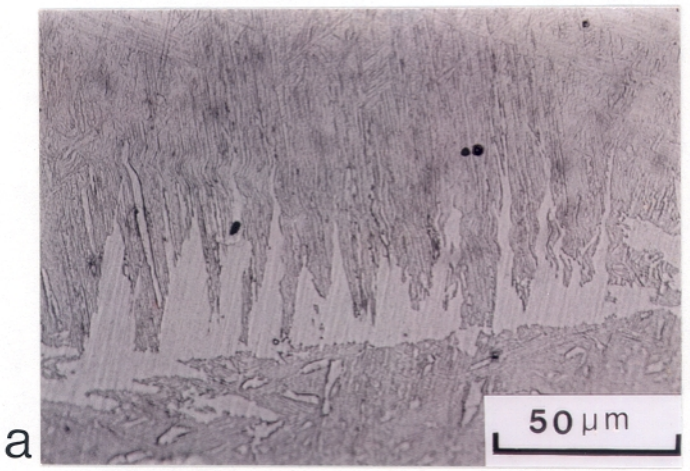

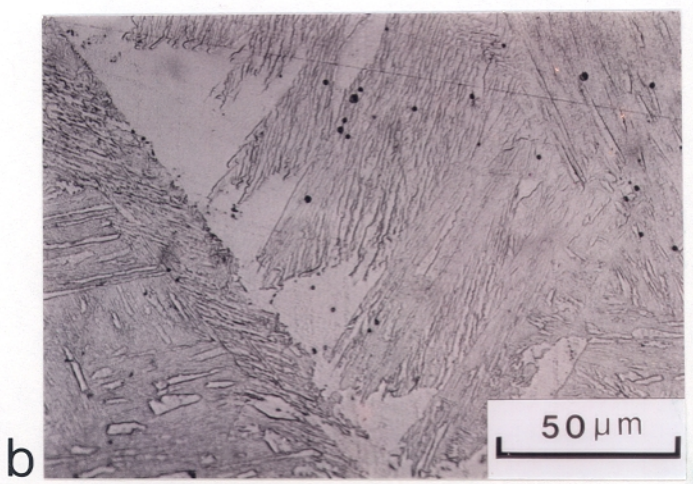

Fig.13 Optical metallographs showing that wedge morphology of Widmanstätten ferrite has become wave-shaped (a), and that Widmanstätten ferrite/austenite interfaces have been degenerated into perturbations (b).

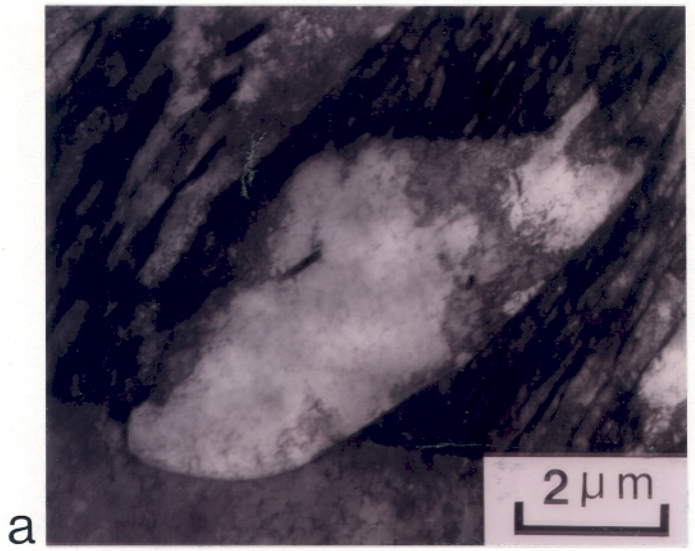

Fig. 14 Transformation electron micrographs (a) and (b) revealing the degenerated interface structures for the corresponding optical metallograph of Fig. 13 (b).

Table 1 Experimental data for the calculation of dislocation density, obtained from the the samples without applied stress.

Two-beam Condition g	No. of Extinction Fringes η_g	Thickness of Thin Foil t(Å)	Measured Dislocation Density (m^{-2})	Corrected Dislocation Density (m^{-2})
<112>	4	2152	8.60×10^{13}	1.15×10^{14}
<112>	4	2152	9.26×10^{13}	1.23×10^{14}
<110>	5	1445	1.49×10^{14}	2.98×10^{14}
<110>	5	1445	1.89×10^{14}	3.78×10^{14}
<110>	6	1734	1.40×10^{14}	2.80×10^{14}
<110>	5	1445	1.14×10^{14}	2.28×10^{14}
<110>	5	1445	1.49×10^{14}	2.98×10^{14}
<112>	4	2152	7.61×10^{13}	1.01×10^{14}
<110>	5	1445	2.03×10^{14}	4.06×10^{14}
<110>	5	1445	1.78×10^{14}	3.56×10^{14}

Table 2 Experimental data for the calculation of dislocation density, obtained from the the samples with applied stress..

Two-beam Condition g	No. of Extinction Fringes η_g	Thickness of Thin Foil t(Å)	Measured Dislocation Density (m^{-2})	Corrected Dislocation Density (m^{-2})
<110>	6	1734	1.65×10^{14}	3.30×10^{14}
<110>	6	1734	1.56×10^{14}	3.12×10^{14}
<110>	6	1734	1.15×10^{14}	2.30×10^{14}
<110>	6	1734	1.65×10^{14}	3.30×10^{14}
<110>	6	1734	1.85×10^{14}	3.70×10^{14}
<110>	6	1734	1.93×10^{14}	3.86×10^{14}
<110>	6	1734	1.48×10^{14}	2.98×10^{14}
<121>	4	2152	2.00×10^{14}	2.67×10^{14}
<112>	4	2152	2.17×10^{14}	2.89×10^{14}
<112>	4	2152	1.52×10^{14}	2.02×10^{14}